ELSEVIER

Journal of Hepatology 48 (2008) 486–493

Journal of Hepatology

www.elsevier.com/locate/jhep

Bovine lactoferrin potently inhibits liver mitochondrial 8-OHdG levels and retrieves hepatic OGG1 activities in Long-Evans Cinnamon rats ☆,☆☆

Akihito Tsubota*, Tetsuya Yoshikawa, Koichi Nariai, Makoto Mitsunaga, Yoko Yumoto, Keiko Fukushima, Sadayori Hoshina, Kiyotaka Fujise

Institute of Clinical Medicine and Research (ICMR), Jikei University School of Medicine, 163-1 Kashiwa-shita, Kashiwa, Chiba 277-8567, Japan

***Background/Aims*: To assess the effect of lactoferrin on oxidative liver damage and its mechanism, we used Long-Evans Cinnamon (LEC) rats that spontaneously develop fulminant-like hepatitis and lethal hepatic failure.**

***Methods*: Four-week-old female LEC rats were divided into the untreated and treated groups. The latter was fed bovine lactoferrin at 2% mixed with conventional diet.**

***Results*: The cumulative survival rates were 75.0% vs. 100% at 14 weeks, 37.5% vs. 91.7% at 15 weeks, and 12.5% vs. 91.7% at 16 weeks, respectively, for untreated and treated rats ($P = 0.0008$). The 8-OHdG levels in liver mitochondrial DNA and malondialdehyde in plasma and liver tissues were significantly lower in treated than untreated rats ($P < 0.001$, =0.017 and 0.034, respectively). Mitochondrial DNA mutations were more common in untreated rats. OGG1 mRNA and protein expression levels were significantly lower in untreated than treated rats ($P = 0.003$ and 0.007, respectively). Hypermethylation of the second CpG island located upstream of OGG1 gene was observed in untreated rats.**

***Conclusions*: Our findings indicated that lactoferrin inhibits oxidative liver damage in LEC rats. Lactoferrin could be potentially useful for the treatment of oxidative stress-induced liver diseases.**

***Keywords*: Wilson's disease; 8-OHdG; OGG1; Methylation; CpG island**

1. Introduction

Chronic inflammation caused by microbes or viruses, exposure to chemicals or radiation, or excess intracellular transition metals is characterized by excess production of reactive oxygen species (ROS) [1,2]. Abundant amounts of transition metals, particularly the non-protein-bound form, interact with physiologically produced ROS, catalyze the formation of highly cytotoxic hydroxyl radicals via the Fenton/Harber–Weiss reaction [3,4], and induce certain diseases, such as Wilson's disease (WD). Oxidative stress initiates lipid peroxidation (LPO) chain reactions, thereby disrupting membranes and organelles, and causes protein degradation, DNA breakage, and mutagenic lesions, such as 8-hydroxy-2′-deoxyguanosine (8-OHdG) [5–9], which is a reliable mar-

Received 22 June 2007; received in revised form 5 November 2007; accepted 20 November 2007; available online 27 December 2007
Associate Editor: Y.M. Deugnier

☆ The authors declare that they do not have anything to disclose regarding funding from industries or conflict of interest with respect to this manuscript.

☆☆ *Contract grant sponsor:* This work was supported in part by a Grant-in-Aid for Scientific Research from the Ministry of Education, Culture, Sports, Science and Technology (Japan), and by a Start-Up Fund from Jikei University School of Medicine. The authors have no conflict of interest with bovine lactoferrin or NRL Pharma, Inc. None of the authors is involved in the production of the agent or is a member or shareholder of the corporation.

* Corresponding author. Tel.: +81 4 7164 1111x6601; fax: +81 4 7166 8638.
E-mail address: atsubo@jikei.ac.jp (A. Tsubota).

Abbreviations: LEC, Long-Evans Cinnamon; OGG1, 8-oxoguanine DNA-glycosylase; 8-OHdG, 8-hydroxy-2 f-deoxyguanosine; ROS, reactive oxygen species.

0168-8278/$32.00 © 2007 European Association for the Study of the Liver. Published by Elsevier B.V. All rights reserved.
doi:10.1016/j.jhep.2007.11.013

ker of ROS-induced DNA modifications. The resulting oxidative modifications could contribute to the pathologic processes in various diseases including cancer.

Long-Evans Cinnamon (LEC) rats, an animal model of WD, are a mutant strain of wild-type Long-Evans Agouti (LEA) rats that have a genetic deletion in the copper-transporting ATPase gene, homologous to the human WD gene. The genetic deficit results in functional failure in the efflux of copper from cells, with resultant accumulation of copper in the liver [10–12]. Based on the copper toxicity, LEC rats are spontaneously predisposed to fulminant-like hepatitis around 4 months of age, which is fatal in 40–50% of them. Surviving rats develop chronic hepatitis and eventually hepatic tumors, one year later. The levels of ROS, LPO and oxidative DNA damage/adducts increase in the liver of LEC but not of LEA rats, in an age- and copper-dependent manner, induce apoptosis, and reach peak levels during the fulminant-like hepatitis period [8,9]. LEC rats represent a suitable animal model for investigating oxidative stress-induced liver injury and subsequent events.

Lactoferrin, a member of the transferrin family, is an iron-binding glycoprotein present in serum and exocrine secretions [13–15]. Lactoferrin is considered to play versatile roles in immune responses and protection against various infections [13–15]. Moreover, various physiological properties and bioactivities have been attributed to lactoferrin, such as anti-oxidative and anti-carcinogenic effects [13–16]. However, the mechanisms behind the functions are not fully understood. In this study, we investigated the mechanism underlying the effect of lactoferrin on oxidative liver injury and subsequent events using LEC rats.

2. Materials and methods

2.1. Animals and treatments

Four-week-old female LEC rats (Charles River Japan, Yokohama, Japan) were maintained in controlled rooms. Animals in the "untreated" group were fed commercial chow, containing 11.0-ppm copper. Animals in the "treated" group received iron-unsaturated bovine lactoferrin (bLF; 94.2% purity, 3% iron saturation; NRL Pharma, Kawasaki, Japan) at 2% mixed with the diet. First, to determine the effect of bLF on hepatic function and survival, 20 LEC rats were subdivided into the untreated ($n = 8$) and treated ($n = 12$) groups. Serum concentrations of aspartate aminotransferase (AST), alanine aminotransferase (ALT) and total bilirubin (T-Bil) were regularly measured. Next, to investigate the mechanism of action, another group of LEC rats ($n = 24$) were divided equally into two groups, and later sacrificed by exsanguination under pentobarbital anesthesia at 13–16 weeks of age. Blood and liver samples were subjected to the following investigations. All experimental protocols were approved by the Committee for the Care and Use of Laboratory Animals of the Jikei University School of Medicine.

2.2. Measurement of copper concentrations

HNO_3/H_2O_2 (4:1) solution was added to acid-cleaned vessels containing the liver samples for microwave digestion. Serum samples were added to 4.5 volumes of 0.1 N HCl. Copper concentrations were measured by the Z-6100 polarized Zeeman atomic absorption spectrophotometer (Hitachi, Tokyo, Japan).

2.3. Histology

Liver specimens were fixed in 10% formalin and embedded in paraffin. The cut sections were stained with hematoxylin and eosin, and for copper with 5(*p*-dimethylaminobenzylidene)rhodamine. Copper-positive cells were counted in four random microscopic fields at 200× magnification.

2.4. Electron microscopy

After perfusion of 2% glutaraldehyde via the portal vein, liver samples were cut into 1 mm cubes and fixed according to conventional procedures. Fine sections of Epon-embedded samples were stained with uranyl acetate and lead citrate, and examined with the H-7500 transmission electron microscope (Hitachi).

2.5. Measurement of malondialdehyde

As a marker of LPO, we measured malondialdehyde (MDA) levels in plasma and liver samples using the Bioxytech MDA-586 kit (OXIS Inc., Portland, OR).

2.6. Measurement of 8-OHdG in nDNA and mtDNA of liver

Nuclear DNA (nDNA) was isolated from liver tissue using the DNA Extractor WB Kit (Wako, Osaka, Japan). Mitochondrial DNA (mtDNA) was isolated using the mtDNA Extractor CT Kit (Wako). To prevent artificial oxidation through air exposure, all solutions and instruments were purged with argon gas. Each extracted DNA was treated with CH_3COONa and nuclease P1 for digestion, and Tris–HCl and alkaline phosphatase for hydrolysis. Aliquots of solutions were used for determination of 8-OHdG using a competitive enzyme-linked immunosorbent assay (Japan Institute for the Control of Aging, Fukuroi, Japan).

2.7. Sequence analysis of mtDNA

Isolated mtDNA was subjected to PCR amplification using overlapping primer sets to span the entire mitochondrial genome (16,319 bases). Conventional PCR was performed in a PCR amplification system. PCR products were sequenced with a DNA analyzer and a dye sequencing kit. The entire sequence of mtDNA was examined for each untreated rat, treated rat and LEA rat. LEA rats ($n = 5$) served as wild-type control and were a gift from Dr. Kozo Matsumoto (Tokushima University, Japan).

2.8. Quantification of OGG1 mRNA by two-step RT-PCR

Total RNA was extracted from fresh liver specimens using the RNeasy Mini Kit (Qiagen, Hilden, Germany). cDNA was synthesized using RNase inhibitor, oligo-$(dT)_{20}$ primer and reverse transcriptase. The sequences of the primers and probe for OGG1 quantification were 5′-CACCCAAGTCAGAAAGGCTTAAC-3′,5′-CCCTGTTGTAAA ACCTGACTTTGA-3′, and TaqMan probe, 5′-FAM-TTCCTACCT CCAAGGCAAACATCCCAA-TAMRA-3′. Real-time PCR was performed using the QuantiTect Probe PCR Kit (Qiagen) and ABI PRISM 7700 Sequence Detection System (Applied Biosystems, Foster City, CA). The resulting data were presented as the normalized quotient, which was derived by dividing the copy numbers of the OGG1 gene by those of the 18S rRNA gene.

2.9. Western blot analysis

Liver tissue was lysed in lysis buffer and sonicated. After centrifugation, proteins were subjected to SDS–polyacrylamide gel electrophoresis, and electrotransferred onto a nitrocellulose membrane. Membranes were blocked with 5% nonfat milk, and probed with primary antibodies. Horseradish peroxidase-labeled secondary antibodies were used for signal detection and blots were visualized with Enhanced Chemiluminescence Western blotting detectionreagents (Amersham Pharmacia Biotech, Piscataway, NJ) and recorded on X-ray film. The primary antibodies used were OGG1/2 (Santa Cruz Biotechnology, Santa Cruz, CA) and β-actin (Abcam, San Diego, CA). The intensity of the scanned image was analyzed using the NIH Image J program. The resulting data were presented as the normalized quotient, which was derived by dividing the intensity of OGG1 by that of β-actin.

2.10. Methylation of CpG island located upstream of OGG1 gene

The $NaHSO_3$ treatment-sequencing procedure [17] was performed to identify the methylation status of all CpG sites in the second CpG island [18] located upstream of OGG1 gene (bases −501 to −178, relative to the start of transcription), which was predicted using MethPrimer (http://www.urogene.org/methprimer/). Denatured DNA was amplified by nested PCR with two primer sets. The sequences of outer primers were 5′-ACACCAAAAGCCCTGAAATG-3′ and 5′-ACCCA GAACGTAGCACCTTG-3′. The sequences of inner primers were 5′-AAAAGTTTTGAAATGGCAGAGCAGGG-3′ and 5′-CTTTCCTT TAAAAAAGCCTCCAGCT-3′. PCR conditions consisted of 35 cycles of 95 °C for 30 s, 54, 56, 58, 60 °C each for 30 s, and 72 °C for 2 min. PCR products were sequenced with the inner primers and dye sequencing kit on the DNA sequencer. This procedure results in the conversion of unmethylated cytosine to thymine, but does not affect the methylated cytosine.

2.11. Measurement of caspase-3 activity

Activity of caspase-3 was measured by the Caspase Fluorometric Assay kit (R&D systems, MN). Fresh liver tissue was homogenized in lysis solution. The plates containing the lysates and reaction buffer were incubated with caspase-3-specific fluorescent substrate, and were read in a fluorescence microplate reader. The resulting data were presented as the normalized quotient, which was derived by dividing values of LEC rats by those of control.

2.12. Statistical analysis

Differences in biochemical indices between two groups were examined by two-way ANOVA of repeated measurements followed by *t* test. Cumulative survival rates were calculated using the Kaplan–Meier method, and differences were analyzed using the log-rank test. Each numerical data set was evaluated for normality of distribution by the Kolmogorov–Smirnov test. The Mann–Whitney test or *t* test was used for comparisons between two groups, and the Bonferroni test or Steel–Dwass test between three groups. All *P* values were two tailed, and values less than 0.05 were considered significant. All analyses were performed using the SPSS 15.0 statistical package (SPSS, Chicago, IL).

3. Results

3.1. Liver function, lethal hepatic failure and morphology

Seven of 8 untreated rats died of hepatic failure between 13.3 and 15.3 weeks of age. In contrast, only 2 of 12 treated rats died of hepatic failure at 15.0 and 19.6 weeks of age. The difference in survival rate between the treated and untreated rats was significant ($P = 0.0008$, Fig. 1). T-Bil concentrations continued to increase in the untreated group, whereas those of the treated group reached a plateau and subsequently decreased ($P = 0.030$ at week 15, Fig. 2A). The mean values of AST and ALT in the treated group were lower at most time points compared with those of the untreated group, albeit statistically insignificant (Fig. 2B).

The median copper concentrations of liver samples were 212.7 μg/g wet weight (range, 183.8–322.5) in the untreated group, and 235.4 μg/g wet weight (168.6–337.9) in the treated group ($P = 0.81$). Serum copper concentrations were 46–320 μg/dL (median, 90) in the untreated group, and 20–388 μg/dL (133) in the treated group ($P = 0.78$).

Hepatocellular pleomorphism and microvesicular steatosis were prominent on specimens from the untreated group (Fig. 3A). Pronounced cellular disarray, including enlarged hepatocytes and variable-size nuclei, was observed in most cases. Lipid droplets of variable size occupied the cytoplasm of many hepatocytes. Spotty necrosis and sinusoidal mononuclear cell and neutrophil infiltrates were scattered in certain lobules. In contrast, specimens of the treated group showed a comparatively lower degree of hepatocellular irregularity and steatosis (Fig. 3B). However, there were no significant differences in the number of copper-stained lesions and the degree of copper staining between the two groups (data not shown).

Mitochondria in the untreated group (Fig. 4A) were enlarged or swollen, and their density was higher compared with those of the treated group (Fig. 4B). Cristae in mitochondria of the untreated group were scanty in number, and radially and peripherally arranged, or became obscure or absent. The membranes of certain mitochondria were obscure. However, the treated group

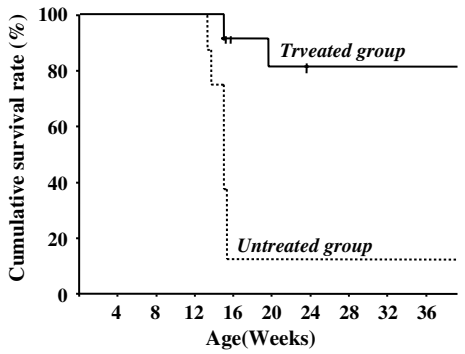

Fig. 1. Cumulative survival rates of untreated and treated rats. The cumulative survival rates were 75.0% vs. 100% at 14 weeks, 37.5% vs. 91.7% at 15 weeks, and 12.5% vs. 91.7% at 16 weeks, of untreated and treated rats, respectively ($P = 0.0008$).

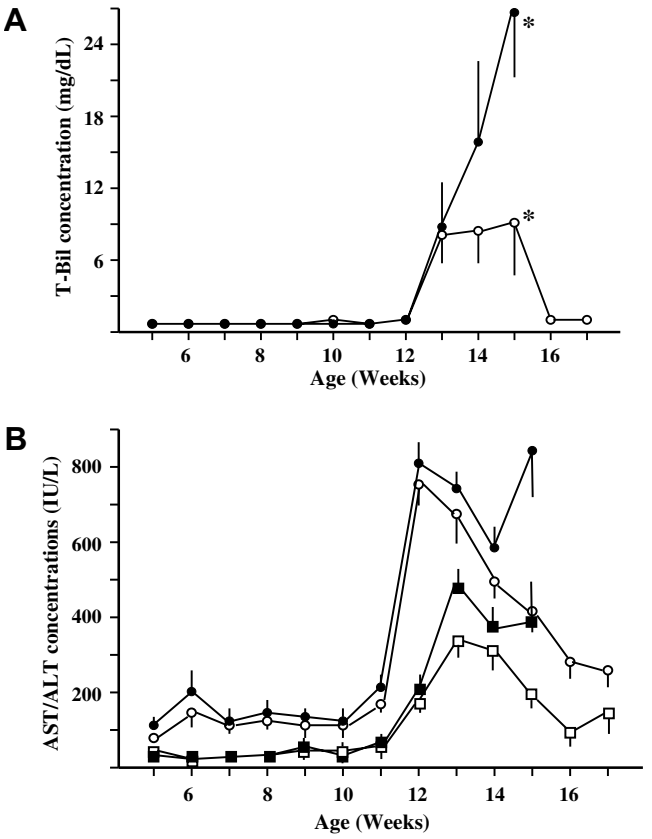

Fig. 2. Time course of changes in biochemical indices. (A) Serum T-Bil concentrations in untreated (closed circles) and treated rats (open circles). *$P = 0.030$. (B) Serum AST and ALT concentrations in untreated rats (closed circles and squares, respectively) and treated rats (open circles and squares, respectively). Data are means ± SEM.

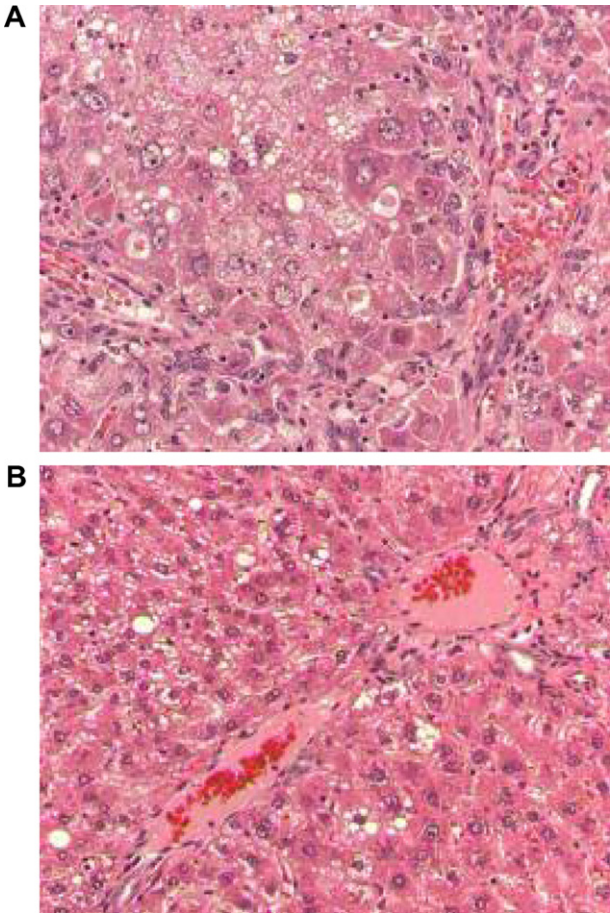

Fig. 3. Histological examination of liver specimens. (A) A representative rat of the untreated group. Note the hepatocellular pleomorphism and marked microvesicular steatosis. (B) A representative rat of the treated group. Note the mild hepatocellular irregularity and steatosis. Hematoxylin and eosin stain, magnification 100×.

showed no or lower degree of these morphological variations.

3.2. Oxidative marker and DNA damage

Plasma MDA levels were significantly higher in the untreated group than treated and control groups ($P = 0.017$ and 0.002; Fig. 5), but there was no significant difference between the treated group and control ($P = 0.380$). Similarly, the MDA levels in liver samples were significantly higher in the untreated group than treated and control groups ($P = 0.034$ and <0.001; Fig. 5), and there was a significant difference between the treated group and control ($P = 0.011$).

The levels of 8-OHdG in nDNA were significantly higher in untreated and treated rats compared with the control (both for $P = 0.004$; Fig. 6), and there was a significant difference in their levels between the untreated and treated groups ($P = 0.021$). Of note, the levels of 8-OHdG in mtDNA were significantly higher in the untreated group than treated and control rats ($P = 0.004$ and <0.001; Fig. 6). The 8-OHdG levels of the treated group were not significantly different from control.

The entire mitochondrial genomes were sequenced from each one sample of the two groups and control. Compared with the prototypical mtDNA sequence of *Rattus norvegicus* (Accession No. NC_001665), several common variations were found among all or most of the samples analyzed (data not shown). Since the common variations possibly arose from different strains, the control sequence was also considered as the consensus sequence. In one treated rat, no mutation was detected throughout the genome sequence (Fig. 7). In contrast, 9 nucleotide substitutions (4 in 12S rRNA, 2 in COX1, 1 in ND3, and 2 in D-loop) were detected in one untreated rat. Next, we sequenced the 12S rRNA and D-loop genome regions from each of 6 liver tissues of both treated and untreated groups (Fig. 7). In all treated rats, no mutation was observed in the 12S rRNA region. Each of two rats showed a single mutation in the D-loop region. In contrast, 5 of the 6 untreated rats had 1–4 mutations in the 12S rRNA region ($P = 0.007$) and 1–8 mutations in the D-loop region ($P = 0.029$).

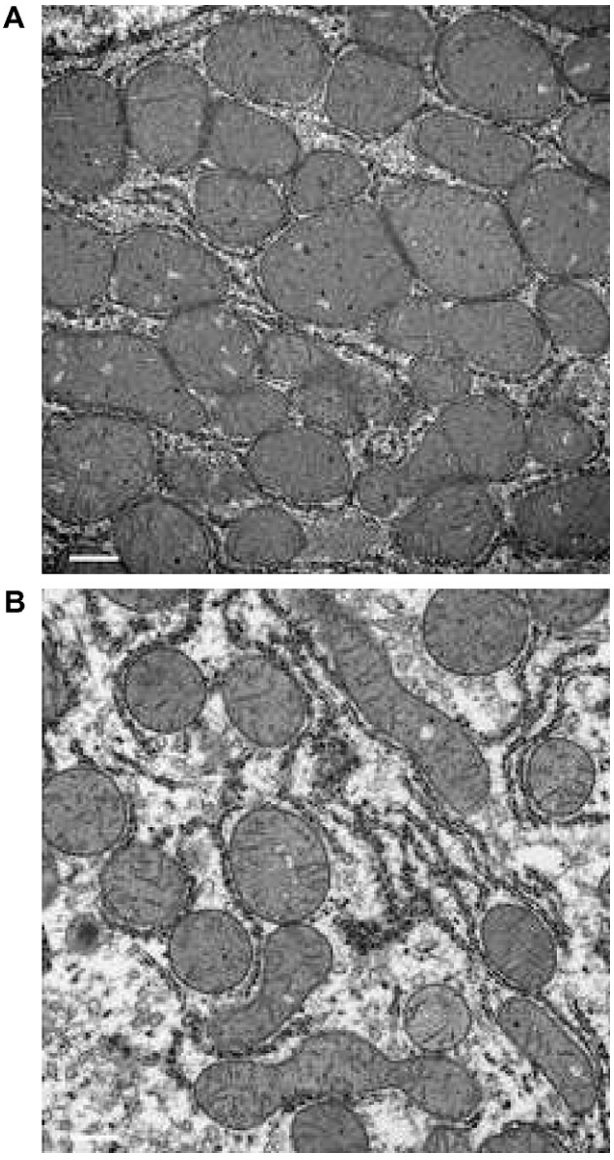

Fig. 4. Transmission electron micrograph of mitochondria in liver specimens. (A) Untreated rat. Note the enlarged/swollen mitochondria, with radially and peripherally arranged cristae, or with obscure or absent cristae. (B) Treated rat. Note the lack of such morphological changes in the mitochondria. Scale bars = 500 nm.

3.3. Expression of OGG1 and methylation of CpG island

The OGG1 mRNA levels in the liver of the treated group were significantly higher than the untreated group ($P = 0.003$) and control ($P = 0.015$; Fig. 8). There was no significant difference between the untreated and control rats. Western blot analysis showed that the expression levels of OGG1 protein were significantly higher in intensity in the treated group than the untreated group ($P = 0.007$) and control ($P = 0.029$; Fig. 9A and B).

The second CpG island contains 25 CpG sites. After $NaHSO_3$-treatment procedures, the CpG sites with or without methylation were successfully determined by direct sequencing in 10 untreated and 8 treated rats. These sequences revealed varying degrees of methylation and methylation patterns among the samples (Fig. 10). In all untreated rats analyzed, all of the 25 CpG sites showed 60–90% of methylation. In contrast, 11 of the 25 sites showed 87–100% of unmethylation, whereas the remaining 14 sites were methylated (63–87%; $P < 0.001$).

The levels of caspase-3 were significantly higher in the untreated group (range, 1.66–6.47; median, 3.17) than the treated group (1.04–2.71; 1.87; $P = 0.039$).

4. Discussion

Our results demonstrated a prominent increase of 8-OHdG in mtDNA in untreated rats, indicating that bLF can potently inhibit oxidative DNA damage especially in the mitochondria. One possible mechanism for this action might be the ability of LF to bind transition metal ions, and thus allowing the transport and delivery of copper to cells similar to iron [19]. Since bLF is 22% saturated with iron in milk, bLF used in this study was nearly equivalent to apo-bLF, which has stronger bioactivities than holo-LF [15,20].

A considerable part of orally administered LF survives gastric digestion *in vivo* [21]. Intact LF diffuses through intestinal mucosal epithelial cells and is transported into blood circulation via the thoracic lymph duct in adult rats [22]. The transporting system within cells is either non-selective or specific receptor-mediated transcytosis. Intact LF in the circulation is rapidly cleared by hepatic parenchymal cells and possibly enters the entero-hepatic circulation. Indeed, the immunoreactive LF content in the liver was 14.4–58.8 ng/g wet weight which is considerably higher than in other organs in treated rats, but was <5 ng/g wet weight in untreated rats (unpublished data), a level similar to that reported in other studies [23,24]. Intact LF bound to the cell surface or internalized into cells could trigger certain signaling pathways or directly activates nuclear DNA as a transcription factor [15,24]. Our study did not examine whether intact LF altered Cu^{+}/Cu^{2+} status in hepatocytes, and certain functions other than just simple metal chelation could not be excluded in the inhibition of oxidative DNA damage.

Oxidized base (purine) lesions are eliminated from the DNA by the base excision repair (BER) pathway, which is initiated by DNA-glycosylase/AP-lyase (OGG1; 8-oxoguanine DNA-glycosylase), a potentially protective cellular mechanism [25,26]. Lack or reduction of the repair capacity would facilitate accumulation of oxidative DNA damage. In LEC rats, both the activity and expression of OGG1 were markedly reduced during fulminant-like hepatitis, suggesting that the liver is poorly protected against oxidative stress. Indeed, the mutagenic

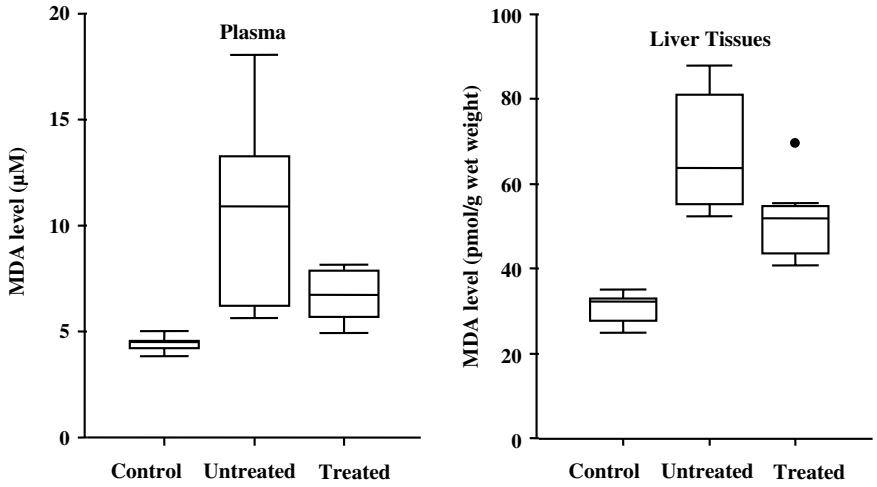

Fig. 5. Malondialdehyde (MDA) levels in plasma and liver tissues of control, untreated and treated rats. *Plasma:* The MDA level in untreated rats was significantly higher (range, 5.64–18.04 μM; median, 10.79) than those in treated (4.94–8.13 μM; 6.73; $P = 0.017$) and control rats (3.83–5.04 μM; 4.49; $P = 0.002$). There was no significant difference between the treated and control rats ($P = 0.380$). *Liver tissues:* The MDA level was significantly higher in untreated (range, 52.31–87.74 pmol/g wet weight; median, 63.84) than in both treated (40.73–72.67 pmol/g wet weight; 52.04; $P = 0.034$) and control rats (25.32–35.47 pmol/g wet; 32.37; $P < 0.001$). There was also a significant difference between treated and control rats ($P = 0.011$). Data are shown as box-and-whisker plot profiles. The bottom and top edges of the boxes represent the 25th and 75th percentiles, respectively. Median values are represented by the line within the box. The whiskers stretch from the boxes to the maximum and minimum values.

oxidized DNA adducts reached peak levels during the period [27]. The low capacity of repair of excess oxidative mtDNA damage might correlate with the low survival rate of untreated rats. Both the mRNA and protein expression levels of OGG1 were higher in treated rats, indicating that LF could recover the impaired BER capacity caused by downregulation of OGG1 expression.

It is not fully known how the epigenetic nature affects the regulatory mechanisms of OGG1 expression. Our study demonstrated that the methylation status of CpG sites in the upstream region of the OGG1 gene could be associated with the OGG1 expression level. The CpG island analyzed was located relatively upstream from 5′-site of the promoter gene but probably overlapped it, which is not yet precisely identified in the rat species. The correlation between oxidative stress and CpG island methylation remains unclear, and it is unknown how methylation is initiated, maintained, or re-converted to the original de-methylation condition.

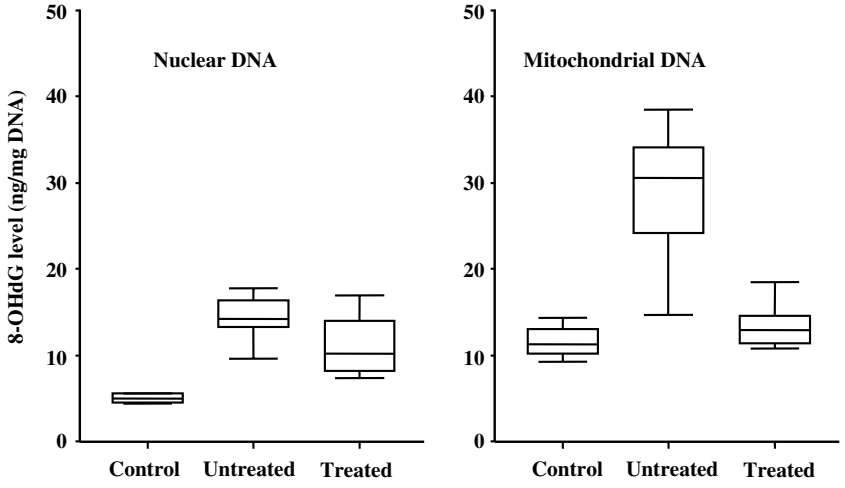

Fig. 6. Accumulation of 8-OHdG in nuclear and mitochondrial DNA extracted from the livers of control, untreated and treated rats. *Nuclear DNA:* 8-OHdG levels were significantly higher in both untreated and treated rats (range, 9.6–17.8 and 7.4–16.9 ng/mg DNA; median, 14.2 and 10.2, respectively), compared with the control (4.4–5.6 ng/mg DNA; 5.0; $P = 0.004$, each). There also was a significant difference between untreated and treated rats ($P = 0.021$). *Mitochondrial DNA:* 8-OHdG levels were significantly higher in untreated (range, 14.7–38.5 ng/mg DNA; median, 30.6) than in control (9.3–14.4 ng/mg DNA; 11.3; $P = 0.004$) and treated rats (10.7–18.5 ng/mg DNA; 12.9; $P < 0.001$). However, the 8-OHdG level in treated rats was not significantly different from that in the control.

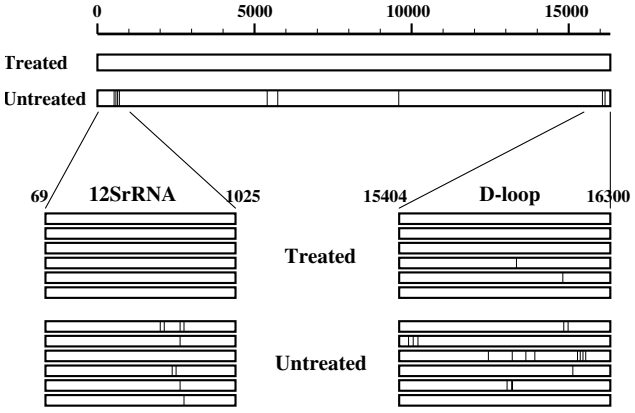

Fig. 7. Mutations in the mitochondrial DNA genome. First, the entire genome sequences were analyzed in each rat of the untreated and treated groups. Next, the 12S rRNA and D-loop genes were sequenced in each of the six rats. Short vertical bars within horizontally long boxes indicate nucleotide mutations.

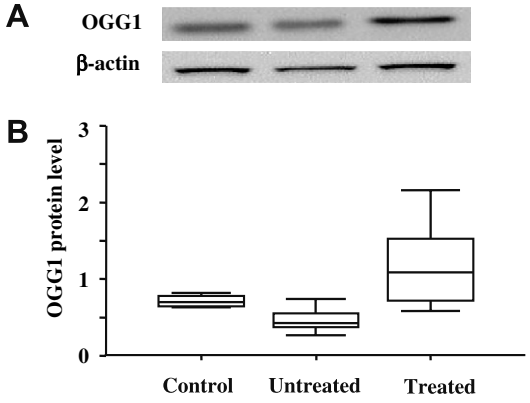

Fig. 9. Expression levels of OGG1 protein by Western blot analysis. (A) Photographs show representative bands for OGG1 and β-actin proteins in each group. (B) Box-and-whisker plot profiles show expression levels of OGG1 protein, depicted as normalized quotient calculated by dividing the band intensities of OGG1 by those of β-actin. The expression level of OGG1 protein in treated rats (0.57–2.23; 1.16) was significantly higher than in the untreated (0.26–0.74; 0.43, $P = 0.007$) and control rats (0.60–0.83; 0.73, $P = 0.029$).

Further studies are warranted to map the methylation status of CpG sites in an extended region, and to determine which methylation of CpG sites critically suppresses the gene expression.

The rise and persistence of oxidative mtDNA damage correlate well with apoptosis [28]. Epigenetic inactivation of OGG1 and increased mutagenic lesions such as 8-OHdG would contribute to increased mtDNA mutations and subsequent apoptosis, resulting in lower survival rates of untreated rats, because mtDNA mutations generate abnormal proteins and impair respiratory chain function, leading to increased ROS production, deterioration of ATP synthesis, and cell death [29]. Few mutations were observed in mtDNA from treated rats, supporting that LF could inhibit oxidative DNA modifications, mtDNA mutations and caspase-3 levels. It is of great interest that mutations concentrated in the 12S rRNA gene, which is important for the regulation of mitochondrial translation and transcription and is the most conserved region in all vertebrates [30]. Furthermore, components of the mitochondrial ribosome include pro-apoptotic proteins [31,32]. The D-loop region contains the leading-strand origin of replication and the promoters of transcription [33]. Consequently, even small mutations in these regions might influence the prognosis of LEC rats with lethal hepatic failure.

Hepatocellular pleomorphism with microvesicular steatosis was less pronounced in treated rats compared with untreated rats. Conspicuous ultrastructural alterations of the mitochondria that are a major target of copper toxicity, together with rearrangement and disappearance of cristae, were displayed in untreated rats, as reported elsewhere [34]. These findings and

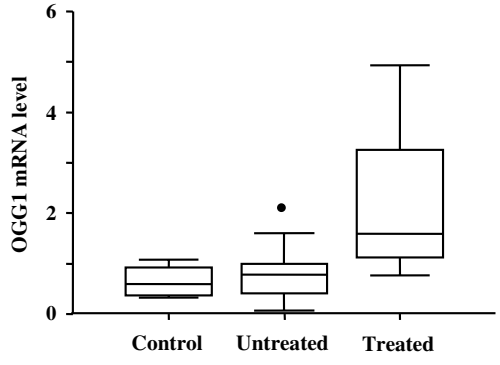

Fig. 8. Quantification of OGG1 mRNA by real-time PCR. The OGG1 mRNA level in treated rats (range, 0.77–4.93; median, 1.59) was significantly higher than that in the control (0.32–1.08; 0.60, $P = 0.015$) and untreated rats (0.07–2.89; 0.78, $P = 0.003$). The mRNA expression level is presented as the ratio of the copy number of OGG1 fragment normalized over that of β-actin. Data are shown as box-and-whisker plot profiles.

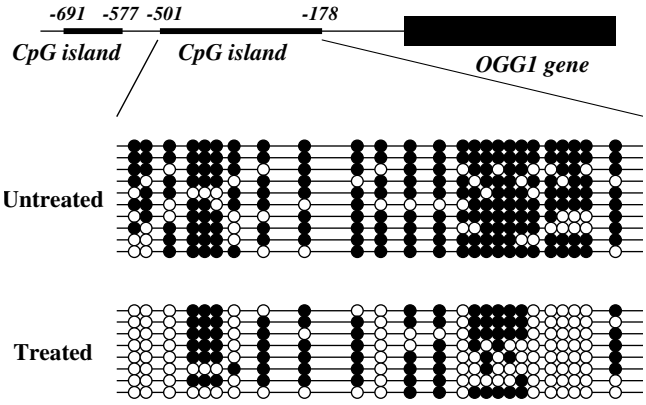

Fig. 10. Methylation of CpG island located upstream of OGG1 gene. The second CpG island contains 25 CpG sites. Methylated and unmethylated CpG sites are denoted by closed and open circles, respectively.

results of MDA support the action of LF as an anti-oxidant lipid protector [14], and accord with a previous report that the severity of ultrastructural changes correlated with the degree of icterus in LEC rats [34]. Although the mechanism that explains the correlation is not clear at this stage, there is no doubt that mitochondria play a critical role in cell and/or individual survival.

In conclusion, LF could recover the impaired BER capacity caused by downregulation of OGG1 expression, and reduce the accumulation levels of 8-OHdG and mutations in hepatic mtDNA, possibly thereby rescuing LEC rats from lethal hepatic failure. LF could be potentially useful for the treatment of oxidative stress-induced liver diseases.

References

[1] Chapple IL. Reactive oxygen species and antioxidants in inflammatory diseases. J Clin Periodontol 1997;24:287–296.

[2] Hensley K, Robinson KA, Gabbita SP, Salsman S, Floyd RA. Reactive oxygen species, cell signaling, and cell injury. Free Radic Biol Med 2000;28:1456–1462.

[3] Aust SD, Morehouse LA, Thomas CE. Role of metals in oxygen radical reactions. J Free Radic Biol Med 1985;1:3–25.

[4] Stohs SJ, Bagchi D. Oxidative mechanisms in the toxicity of metal ions. Free Radic Biol Med 1995;18:321–336.

[5] Richter C, Park JW, Ames BN. Normal oxidative damage to mitochondrial and nuclear DNA is extensive. Proc Natl Acad Sci USA 1988;85:6465–6467.

[6] Toyokuni S, Sagripanti JL. Association between 8-hydroxy-2′-deoxyguanosine formation and DNA strand breaks mediated by copper and iron. Free Radic Biol Med 1996;20:859–864.

[7] Hudson EK, Hogue BA, Souza-Pinto NC, Croteau DL, Anson RM, Bohr VA, et al. Age-associated change in mitochondrial DNA damage. Free Radic Res 1998;29:573–579.

[8] Yamamoto H, Hirose K, Hayasaki Y, Masuda M, Kazusaka A, Fujita S. Mechanism of enhanced lipid peroxidation in the liver of Long-Evans cinnamon (LEC) rats. Arch Toxicol 1999;73:457–464.

[9] Nair J, Strand S, Frank N, Knauft J, Wesch H, Galle PR, et al. Apoptosis and age-dependant induction of nuclear and mitochondrial etheno-DNA adducts in Long-Evans Cinnamon (LEC) rats: enhanced DNA damage by dietary curcumin upon copper accumulation. Carcinogenesis 2005;26:1307–1315.

[10] Mori M, Yoshida MC, Takechi N, Taniguchi N. The LEC rat, a new model for hepatitis and liver cancer. Tokyo: Springer-Verlag; 1991, p. 1–356.

[11] Li Y, Togashi Y, Sato S, Emoto T, Kang JH, Takeichi N, et al. Spontaneous hepatic copper accumulation in Long-Evans Cinnamon rats with hereditary hepatitis. A model of Wilson's disease. J Clin Invest 1991;87:1858–1861.

[12] Wu J, Forbes JR, Chen HS, Cox DW. The LEC rat has a deletion in the copper transporting ATPase gene homologous to the Wilson disease gene. Nat Genet 1994;7:541–545.

[13] Baveye S, Elass E, Mazurier J, Spik G, Legrand D. Lactoferrin: a multifunctional glycoprotein involved in the modulation of the inflammatory process. Clin Chem Lab Med 1999;37:281–286.

[14] Kanyshkova TG, Buneva VN, Nevinsky GA. Lactoferrin and its biological functions. Biochemistry 2001;66:1–7.

[15] Legrand D, Elass E, Carpentier M, Mazurier J. Lactoferrin: a modulator of immune and inflammatory responses. Cell Mol Life Sci 2005;62:2549–2559.

[16] Lindmark-Mansson H, Akesson B. Antioxidative factors in milk. Br J Nutr 2000;84:S103–S110.

[17] Clark SJ, Harrison J, Paul CL, Frommer M. High sensitivity mapping of methylated cytosines. Nucleic Acids Res 1994;22:2990–2997.

[18] Gardiner-Garden M, Frommer M. CpG islands in vertebrate genomes. J Mol Biol 1987;196:261–282.

[19] Smith CA, Anderson BF, Baker HM, Baker EN. Metal substitution in transferrins: the crystal structure of human copper-lactoferrin at 2.1-A resolution. Biochemistry 1992;31:4527–4533.

[20] Kruzel ML, Bacsi A, Choudhury B, Sur S, Boldogh I. Lactoferrin decreases pollen antigen-induced allergic airway inflammation in a murine model of asthma. Immunology 2006;119:159–166.

[21] Troost FJ, Steijns J, Saris WH, Brummer RJ. Gastric digestion of bovine lactoferrin in vivo in adults. J Nutr 2001;131:2101–2104.

[22] Takeuchi T, Kitagawa H, Harada E. Evidence of lactoferrin transportation into blood circulation from intestine via lymphatic pathway in adult rats. Exp Physiol 2004;89:263–270.

[23] Ji B, Maeda J, Higuchi M, Inoue K, Akita H, Harashima H, et al. Pharmaco-kinetics and brain uptake of lactoferrin in rats. Life Sci 2006;78:851–855.

[24] Fischer R, Debbabi H, Blais A, Dubarry M, Rautureau M, Boyaka PN, et al. Uptake of ingested bovine lactoferrin and its accumulation in adult mouse tissues. Int Immunopharmacol 2007;7:1387–1393.

[25] Friedberg E, Walker GC, Siede W. Base excision repair. In: Friedberg E, editor. DNA repair and mutagenesis. Washington (DC): ASM Press; 1995. p. 135–169.

[26] Hill JW, Hazra TK, Izumi T, Mitra S. Stimulation of human 8-oxoguanine-DNA glycosylase by AP-endonuclease: potential coordination of the initial steps in base excision repair. Nucleic Acids Res 2001;29:430–438.

[27] Choudhury S, Zhang R, Frenkel K, Kawamori T, Chung FL, Roy R. Evidence of alterations in base excision repair of oxidative DNA damage during spontaneous hepatocarcinogenesis in Long Evans Cinnamon rats. Cancer Res 2003;63:7704–7707.

[28] Asoh S, Mori T, Hayashi J, Ohta S. Expression of the apoptosis-mediator Fas is enhanced by dysfunctional mitochondria. J Biochem 1996;120:600–607.

[29] Wei YH, Lu CY, Lee HC, Pang CY, Ma YS. Oxidative damage and mutation to mitochondrial DNA and age-dependent decline of mitochondrial respiratory function. Ann NY Acad Sci 1998;854:155–170.

[30] Gadaleta G, Pepe G, De Candia G, Quagliariello C, Sbisa E, Saccone C. The complete nucleotide sequence of the *Rattus norvegicus* mitochondrial genome: cryptic signals revealed by comparative analysis between vertebrates. J Mol Evol 1989;28:497–516.

[31] Koc EC, Ranasinghe A, Burkhart W, Blackburn K, Koc H, Moseley A, et al. A new face on apoptosis: death-associated protein 3 and PDCD9 are mitochondrial ribosomal proteins. FEBS Lett 2001;492:166–170.

[32] Suzuki T, Terasaki M, Takemoto-Hori C, Hanada T, Ueda T, Wada A, et al. Proteomic analysis of the mammalian mitochondrial ribosome. J Biol Chem 2001;276:33181–33195.

[33] Taanman JW. The mitochondrial genome: structure, transcription, translation and replication. Biochim Biophys Acta 1999;1410:103–123.

[34] Sternlieb I, Quintana N, Volenberg I, Schilsky ML. An array of mitochondrial alterations in the hepatocytes of Long-Evans Cinnamon rats. Hepatology 1995;22:1782–1787.